



Titan Prebiotic Explorer Study (TiPex)

Balloon Trajectory Simulation Study Final Report

Dr. Alexey Pankine

Global Aerospace Corporation

5 May 2006

NASA JPL PO#: 1282602

GAC Report 140-82602-001



711 W. Woodbury Road, Suite H
Altadena, CA 91001-5327 USA
Telephone: +1 (626) 345-1200
Fax (626) 296-0929
Email: global@gaerospace.com
Web: <http://www.gaerospace.com>

Abstract

Trajectories of constant altitude Titan balloons are simulated with parametric models of zonal and tidal winds for a range of seasons, altitudes and starting latitudes with the goal of quantifying latitudinal coverage achievable with free-floating Titan balloons. For each set of parameters trajectories variability is studied by adding a random component to the wind field and by initiating trajectories at different local hours. Analysis of the simulated trajectories shows that trajectories simulated with weak zonal winds are strongly affected by the tidal wind effects and show the largest latitudinal coverage. Latitudinal ranges covered by trajectories range from 10° to 80° of latitude with the average range of about 30°. All simulated trajectories are bounded within a latitudinal corridor centered near the starting latitude.

TABLE OF CONTENTS

1. INTRODUCTION.....	1
2. STUDY OBJECTIVES AND APPROACH.....	2
3. BALLOON TRAJECTORY SIMULATION MODEL	3
3.1. INTRODUCTION	3
3.2. GENERAL DESCRIPTION OF THE MODEL.....	3
3.3. TRAJECTORY CALCULATION LITERATURE REVIEW	3
3.4. CALCULATION METHODOLOGY	4
4. TITAN WIND MODELS	6
4.1. INTRODUCTION	6
4.2. ZONAL WINDS	6
4.3. TIDAL WINDS.....	9
4.4. RANDOM WIND COMPONENT	12
4.5. PARAMETRIC MODELS WIND FIELDS	13
5. TRAJECTORY SIMULATION RESULTS	15
5.1. INTRODUCTION	15
5.2. TRAJECTORY SIMILARITY	15
5.3. RANGE OF LOCATIONS (LATITUDES).....	15
6. SUMMARY	30
APPENDIX A: EARTH DATES OF TITAN SEASONS.....	31

TABLE OF FIGURES

Figure 4-1. TN05 zonal winds for $L_s=180^\circ$ (Fig. 1 of TN05).....	6
Figure 4-2. Parameterized zonal wind field for $L_s=180^\circ$ based on TN05 results.....	7
Figure 4-3. Parameterized zonal wind field for $L_s=270^\circ$ based on TN05 results.....	7
Figure 4-4. Parameterized zonal wind field for $L_s=0^\circ$ based on TN05 results.....	7
Figure 4-5. Parameterized zonal wind field for $L_s=90^\circ$ based on TN05 results.....	8
Figure 4-6. Parameterized zonal wind field for $L_s=180^\circ$ based on LMD results.....	8
Figure 4-7. Parameterized zonal wind field for, $L_s=270^\circ$ based on LMD results.....	8
Figure 4-8. Parameterized zonal wind field for, $L_s=0^\circ$ based on LMD results.....	9
Figure 4-9. Tidal wind zonal and meridional amplitude variation with altitude (from TN02).....	10
Figure 4-10. Parametric model wind field at 40 km.....	10
Figure 4-11. TN02 wind field at 40 km (Fig. 7 of TN02).....	11
Figure 4-12. Parametric model wind field at 300 m.....	11
Figure 4-13. TN02 wind field at 300 m (Fig. 5 of TN02).....	12
Figure 4-14. Global wind field at 8 km $L_s=180^\circ$ in the parametric model with TN05 zonal winds.....	13
Figure 4-15. Global wind field at 8 km $L_s=270^\circ$ in the parametric model with TN05 zonal winds.....	13
Figure 4-16. Global wind field at 8 km $L_s=270^\circ$ in the parametric model with LMD zonal winds.....	14
Figure 5-1. Simulated trajectories at 18 km, $L_s=270^\circ$ generated with parametric model with TN05 zonal winds.....	16
Figure 5-2. Simulated trajectories at 18 km, $L_s=270^\circ$ generated with parametric model with LMD zonal winds.....	16
Figure 5-3. Simulated trajectories at 1 km, $L_s=270^\circ$ generated with parametric model with LMD zonal winds.....	17
Figure 5-4. Evolution of the shape of a trajectory with varying underlying winds.....	17
Figure 5-5. Simulated trajectories at altitudes of 1, 4, 8, 12 and 18 km, $L_s=270^\circ$, starting latitude of 65° generated with parametric model with TN05 zonal winds.....	19
Figure 5-6. 12 trajectories simulated for different starting local time, for $L_s=270^\circ$, 18 km altitude, parametric model with TN05 zonal winds.....	20
Figure 5-7. Longitudinal envelopes of sets of trajectories initiated at different latitudes and different local times at $L_s=180^\circ$, 18 km altitude, parametric model with TN05 zonal winds.....	21
Figure 5-8. Histograms of latitudes covered by simulated trajectories generated with TN05 zonal wind model with random component for $L_s=270^\circ$, 18 km altitude.....	22
Figure 5-9. Histograms of latitudes covered by simulated trajectories generated for 12 different local hours with TN05 zonal wind model for $L_s=270^\circ$, 18 km altitude.....	23
Figure 5-10. Histograms of latitudes covered by simulated trajectories generated with LMD zonal wind model with random component for $L_s=270^\circ$, 18 km altitude.....	24
Figure 5-11. Latitudinal ranges at different altitudes covered by simulated trajectories generated with TN05 zonal wind model with random component for $L_s=270^\circ$	25
Figure 5-12. Latitudinal ranges at different altitudes covered by simulated trajectories generated for 12 different local hours with TN05 zonal wind model for $L_s=270^\circ$	26
Figure 5-13. Histograms of latitudinal ranges for all altitudes and seasons, for both parametric models (top) for simulations with 12 random trajectories for each starting latitude; (bottom) for simulations with trajectories at 12 different local hours for each starting latitude.....	27
Figure 5-14. Comparison of zonal wind magnitudes in the LMD model for $L_s=270^\circ$ and phase speed magnitude of the tidal wind planetary wave.....	28
Figure 5-15. Comparison of zonal wind magnitudes in the TN05 model for $L_s=270^\circ$ and phase speed magnitude of the tidal wind planetary wave.....	29

Titan Prebiotic Explorer Study (TiPex)

Balloon Trajectory Simulation Study

Final Report

1. Introduction

Future exploration of the Saturn moon Titan may involve “hot air” balloons that circumnavigate the planet at altitudes above the surface between 1 to 20 km and that occasionally descend to the surface to perform surface sample analysis activities. One of the first steps in designing such a mission is to develop an understanding of possible balloon trajectories in the lower atmosphere at relevant altitudes, latitudes and seasons. This study is the first attempt to simulate and analyze balloon trajectories in the lower atmosphere of Titan.

2. Study Objectives and Approach

The objective of this study is to simulate balloon trajectories in the lower atmosphere of Titan and to determine 1) whether the trajectories are very similar to each other, 2) whether the trajectories generally cover a wide or narrow range of locations (latitudes), and 3) whether the trajectories appear to be entirely trapped within a narrow region, e.g., near the pole if started at high latitudes.

Titan balloon trajectories are simulated using Global Aerospace's Trajectory Simulation Model (TSM, see Section 3). Two models of global Titan winds are constructed to provide input for the TSM. These models are constructed by combining parameterized tidal wind fields (based on the general circulation model [GCM] results of Takano and Neubauer, 2002¹, henceforth referred to as TN02) with zonal mean fields; the latter derived from 3-D Takano and Neubauer, 2005 GCM² (henceforth referred to as TN05) and 2-D Laboratoire de Meteorologie Dynamique GCM³ (henceforth referred to as LMD) (see Section 4). For these wind models we include a random component describing variations about mean values.

Trajectories are simulated for 180 Earth days, for constant altitude levels for a range of seasons, latitudes and altitudes. Specifically, trajectories are simulated for a) latitudes -65° , -45° , -25° , 0° , 25° , 45° and 65° ; b) altitudes of 1, 4, 8, 12 and 18 km; and c) seasons corresponding to the longitude of the Sun, $L_s = 180^\circ$, 270° , 0° , and 90° for the model with TN05 zonal winds, and $L_s = 180^\circ$, 210° , 240° , 270° , 300° , 330° , and 360° for the model with LMD zonal winds. In order to assess sensitivity to expected wind variability, for each combination of altitude, latitude and season, 12 trajectories are simulated using the stochastic wind perturbation, 12 trajectories are simulated using mean winds, but for different local times spanning one Titan day (15.9454 Earth days). This effort involves simulating and analyzing a total of 9,240 individual trajectories.

¹ T. Takano and F. Neubauer, "Tidal Winds on Titan Caused by Saturn", *Icarus* 158, 499–515, 2002.

² T. Tokano and F. Neubauer, "Wind-induced seasonal angular momentum exchange at Titan's surface and its influence on Titan's length-of-day", *Geophys. Res. Lett.*, Vol. 32, L24203, doi:10.1029/2005GL024456, 2005

³ "GCM Titan Database", <http://www.lmd.jussieu.fr/titanDbase/index.html>

3. Balloon Trajectory Simulation Model

3.1. Introduction

This section discusses the numerical model used in the simulations of the balloon trajectories. It gives a brief overview of the model, reviews the trajectory calculation literature and presents the calculations methodology.

3.2. General Description of the Model

The numerical model that calculates balloon trajectories assumes that the balloon floats at the velocity of the winds. The model propagates the balloon position through the wind field on a step-by-step basis. This process is repeated until the simulation is complete.

3.3. Trajectory Calculation Literature Review

Although the mathematics of trajectory calculation are simple, several issues influence trajectory accuracy, computational resource requirements, and computational speed. Several papers discuss issues related to trajectory calculation, including integration schemes and interpolation methods.

Seibert⁴ discusses the accuracy of several integration schemes within the context of trajectory calculation using gridded global atmospheric data. Seibert shows conditions for which many integration schemes converge to identical error values.

Traditionally, higher order numerical integration schemes are thought to be superior to lower order schemes because, for the same accuracy, they allow longer time steps. In the case of integration of global, gridded data, the tradeoff is not simple. Seibert notes, “[i]f higher accuracy is demanded, there is always the alternative of using shorter time steps instead of increasing the order of approximation.... If the smallest features resolved by the wind data are to be reproduced in the trajectories, no grid cell must be skipped during a time step of the trajectory computation.” Thus, there is an accuracy tradeoff between the integration order and time step. In fact, higher order integration schemes may be detrimental to computational speed if no grid cell is to be skipped.

Another issue in calculating atmospheric trajectories is the method of interpolation used for estimating off-grid atmospheric data. Staniforth and Côté⁵ indicate that, “[i]n practice however, in the context of both passive advection and coupled systems of equations in several spatial dimensions, it is found... that it is sufficient to use linear interpolation for the computation of the displacements.”

⁴ Seibert, Petra, “Convergence and Accuracy of Numerical Methods for Trajectory Calculations”, *Journal of Applied Meteorology*, Vol. 32, March 1993, pp.558-566.

⁵ Staniforth, Andrew and Jean Côté, “Semi-Lagrangian Integration Schemes for Atmospheric Models—A Review,” *Monthly Weather Review*, Vol. 119, September 1991, pp. 2206–2223.

3.4. Calculation Methodology

For the present study, for simplicity, the balloons are assumed to float at constant altitude. The wind data is interpolated spatially to obtain local conditions at points in the atmosphere. No time interpolation is needed since the zonal wind fields do not change with time in this model and the tidal winds at any moment in time can be calculated exactly from the parametric formulation. The interpolation scheme employed for spatial interpolation is a standard linear interpolation. The corner points of a cell in the atmospheric data are interpolated first in longitude, and then in latitude. The result is that the 4 surrounding points in the atmospheric data set are interpolated to one value to be used in trajectory calculations.

The trajectories evaluated in this study were generated by integrating model winds at the position of the balloon. The derivative of longitude with respect to time is given by

$$\frac{d(lon)}{dt} = \frac{u}{\cos(lat) \frac{D + 2z}{2}}, \quad (1.)$$

where

lon = longitude [rad],

t = time,

u = zonal wind [m/s],

lat = latitude [rad],

D = Titan's diameter [m], and

z = balloon altitude [m].

The derivative of latitude with respect to time is given by

$$\frac{d(lat)}{dt} = \frac{v}{\frac{D + 2z}{2}}, \quad (2.)$$

where

lat = latitude [rad], and

v = meridional wind [m/s].

The derivative of altitude with respect to time is

$$\frac{dz}{dt} = 0, \quad (3.)$$

due to the constant-altitude assumption.

Integrations were performed numerically with a simple, first order scheme, based on the considerations of accuracy and time step as discussed above:

$$y_{i+1} = y_i + \left(\frac{dy}{dt} \right)_i \Delta t, \quad (4.)$$

where

y = an independent variable, longitude, latitude, or altitude,

i = value at “current” time step,

$i+1$ = value at “next” time step, and

Δt = time step [s].

To satisfy the Courant-Friederichs-Lewy criterion:

$$\Delta t < \frac{\Delta x}{|u|}$$

(where Δt is the time step, Δx is the smallest spatial dimension of the data grid and $|u|$ is the largest wind speed magnitude), the time step of the simulation was chosen to be 1 hour. Indeed, LMD mean zonal winds are given with 3.75° resolution in latitude and the maximum magnitude of the zonal winds in the LMD model below 20 km is 25 m/s, while amplitude of the tidal winds does not exceed 4 m/s (see Section 4). Hence,

$$\Delta t_{LMD} < \frac{\Delta x}{|u|} = \frac{1.7 \cdot 10^5}{29} \approx 1.6 \text{ hours.}$$

The mean zonal winds in the parametric model with TN05 zonal winds are given with a resolution of 10° in latitude, while the maximum magnitude of the zonal winds is 4 m/s. Hence, for the parametric model with TN05 zonal winds

$$\Delta t_{TN05} < \frac{\Delta x}{|u|} = \frac{4.5 \cdot 10^5}{8} \approx 15.6 \text{ hours.}$$

4. Titan Wind Models

4.1. Introduction

This section discusses parametric models of Titan winds constructed to simulate trajectories of Titan balloons.

4.2. Zonal Winds

Two models of the zonal winds were developed - one based on parameterization of the TN05 GCM² simulations and one based on parameterization of the LMD GCM³ simulations. Zonal winds in LMD are given as a function of the pressure, rather than altitude. Latitude-pressure profiles of LMD zonal winds were converted to latitude versus geopotential height profiles using interpolation.

Figure 4-1 and Figure 4-2 show zonal wind fields for $L_s = 180^\circ$ from TN05 and from the parameterized model, respectively. As can be seen, the parameterized model captures major features of the zonal circulation. Figure 4-3, Figure 4-4 and Figure 4-5 show zonal wind fields of the parameterized zonal wind model for other seasons.

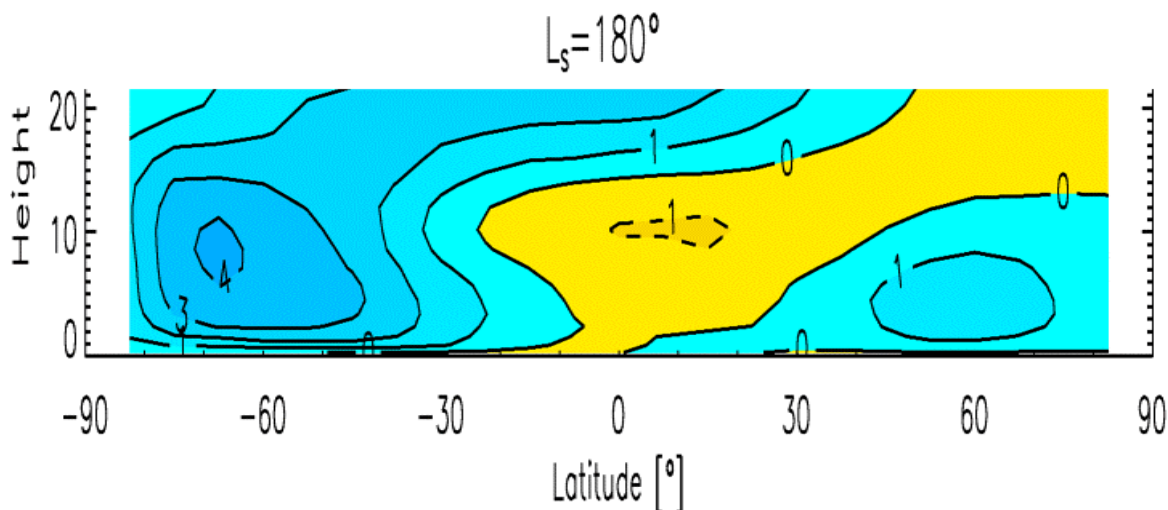


Figure 4-1. TN05 zonal winds for $L_s=180^\circ$ (Fig. 1 of TN05).

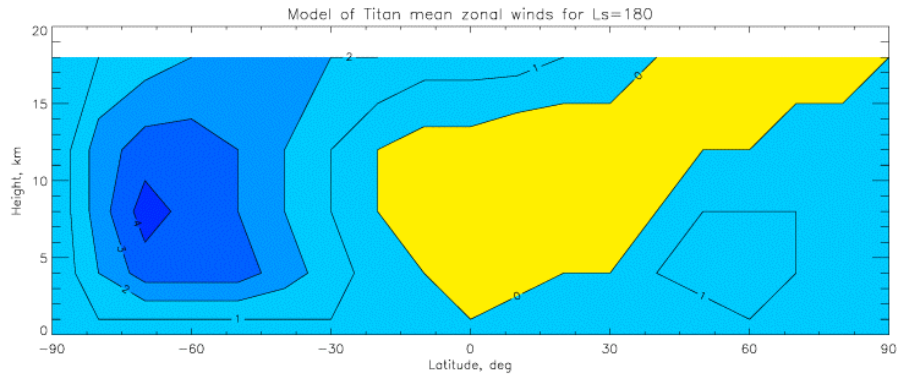


Figure 4-2. Parameterized zonal wind field for Ls=180° based on TN05 results.

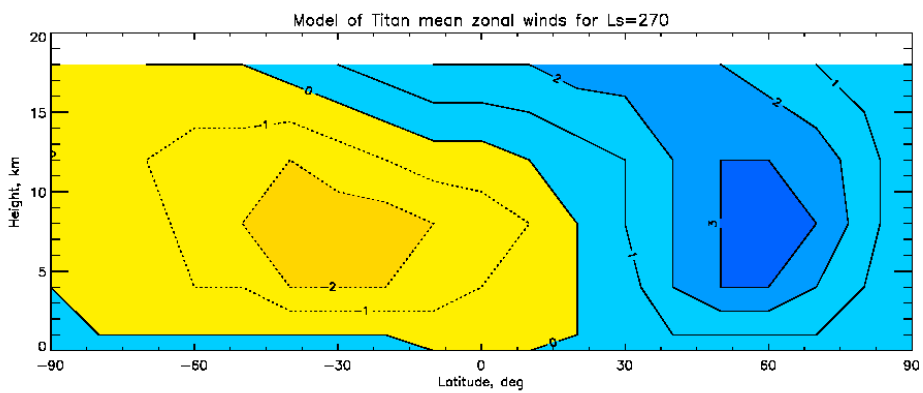


Figure 4-3. Parameterized zonal wind field for Ls=270° based on TN05 results.

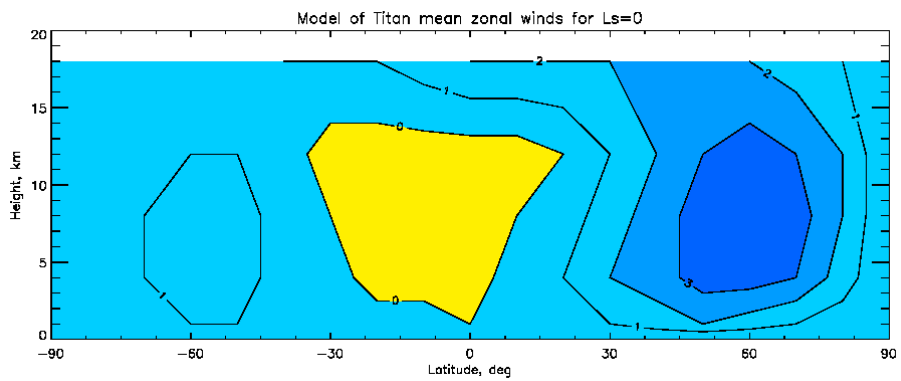


Figure 4-4. Parameterized zonal wind field for Ls=0° based on TN05 results.

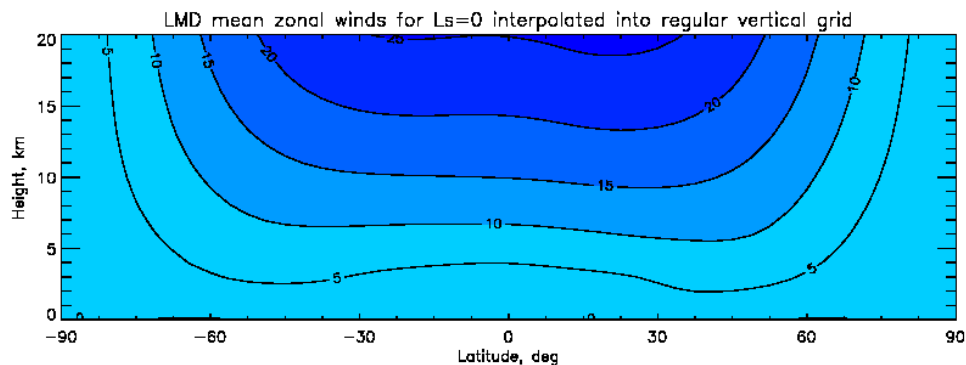


Figure 4-8. Parameterized zonal wind field for, $L_s=0^\circ$ based on LMD results.

4.3. Tidal Winds

Tidal winds are modeled following the TN02 GCM simulations¹. In TN02, Takano and Neubauer note “The tidal flow within the background circulation manifest itself as an eastward traveling planetary-scale wave of wavenumber 2. The waves of the northern hemisphere and southern hemisphere are in phase because the forcing by the tide is symmetric about the equator. The wave migrates eastward without dispersion with half of Titan’s orbital velocity”. In addition, we note that the spatial pattern of the Titan tidal winds is independent of the season, since the rotational axis of Titan and Saturn are parallel. The seasons on Titan arise due to obliquity of the Saturn/Titan equator relative to ecliptic.

In accordance with the description of the tidal flow in TN02, we approximate zonal and meridional tidal winds as:

$$u_t = u_{0t} \cos(2(\varphi - ct)) \cdot \cos(3\theta)$$

$$v_t = v_{0t} \cos(2(\varphi - ct - \pi/4)) \cdot \sin(3\theta)$$

to match the global wind field pattern at 40 km. Here u_t and v_t are the zonal and meridional component of tidal winds (in m/s), respectively; u_{0t} and v_{0t} are amplitudes of the zonal and meridional components; φ is longitude, θ is latitude (90° at North pole; c is the phase velocity of the tidal wave propagation:

$$c = \frac{\pi}{T}$$

where T is Titan orbital period equal to 15.9454 Earth days; and t is time.

Amplitudes u_{0t} and v_{0t} vary with altitude as illustrated in Figure 4-9.

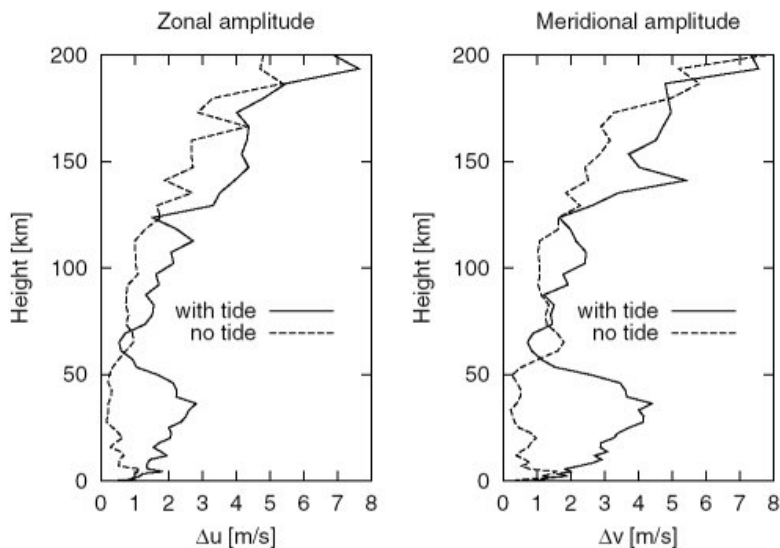


FIG. 9. Vertical profile of the longitudinal amplitude of the zonal (left panel) and meridional (right panel) wind at 60°N simulated by the GCM with and without tide. The difference between the two curves in each panel may be regarded as the oscillation caused by the gravitational tide.

Figure 4-9. Tidal wind zonal and meridional amplitude variation with altitude (from TN02)

We approximate the tidal wind amplitudes dependence on altitude between 0 and 40 km simply as:

$$u_{0t}(z) = 1 + z / 20$$

$$v_{0t}(z) = 1 + z / 10, \text{ for } 0 < z < 30 \text{ and } v_{0t}(z) = 4, \text{ for } 30 < z < 40 \text{ km,}$$

where z is in km, u_{0t} and v_{0t} are in m/s.

This approximation produces a reasonable match to the published Titan wind fields (TN02) and simplifies trajectory simulation.

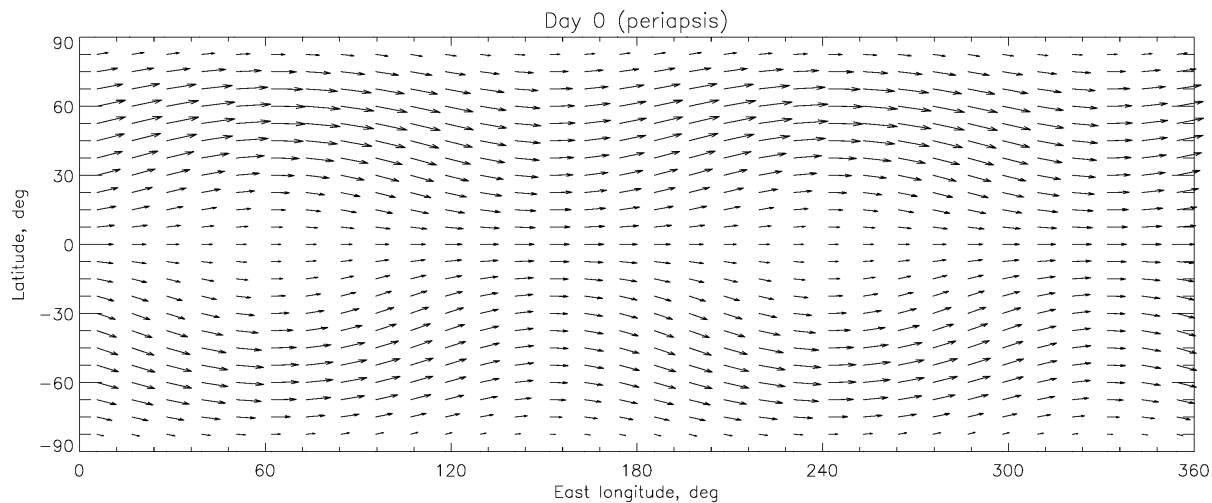


Figure 4-10. Parametric model wind field at 40 km.

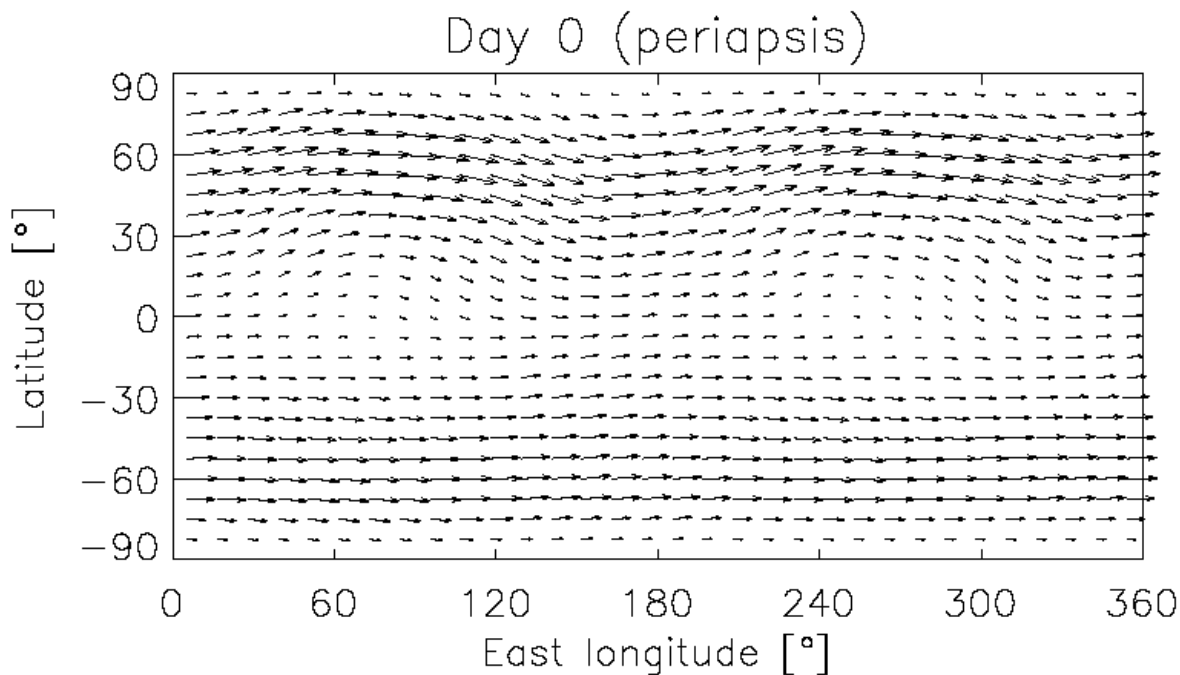


Figure 4-11. TN02 wind field at 40 km (Fig. 7 of TN02).

Figure 4-10 and Figure 4-11 compare Titan wind fields at 40 km generated with a simplified model described above (Figure 4-10) and from TN02 (Figure 4-11). The wind fields represent a sum of the tidal and background zonal winds. The background zonal wind in Figure 4-10 was approximated from the data in TN02 for comparison with the results of TN02.

At low altitudes (300 m) the parametric model fails to reproduce the GCM generated wind field of TN02. Figure 4-12 and Figure 4-13 compare global wind fields at 300 m in the parametric model and in TN02 GCM.

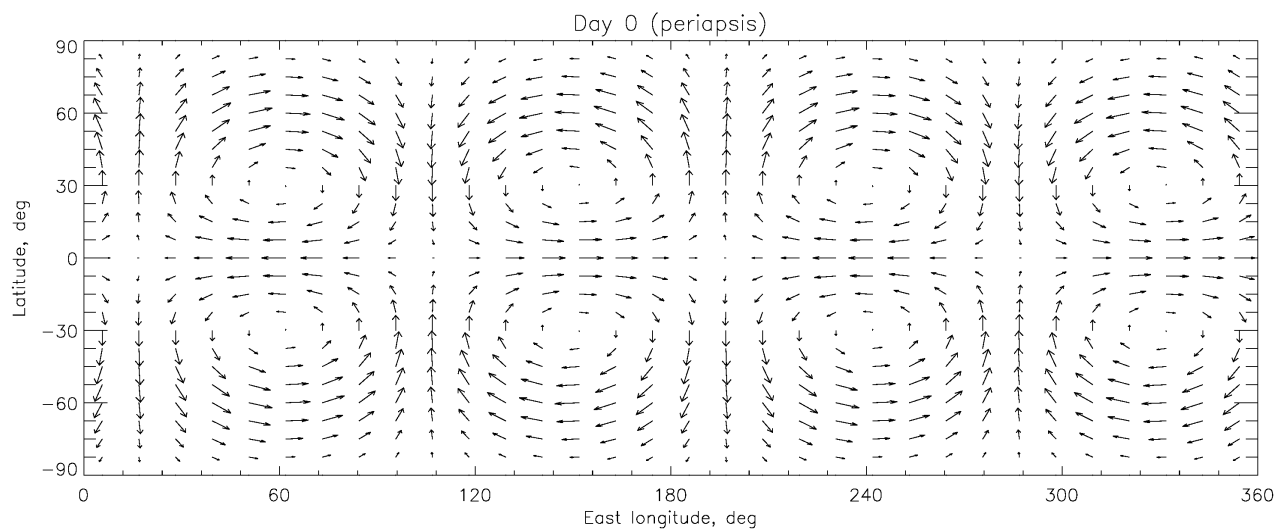


Figure 4-12. Parametric model wind field at 300 m.

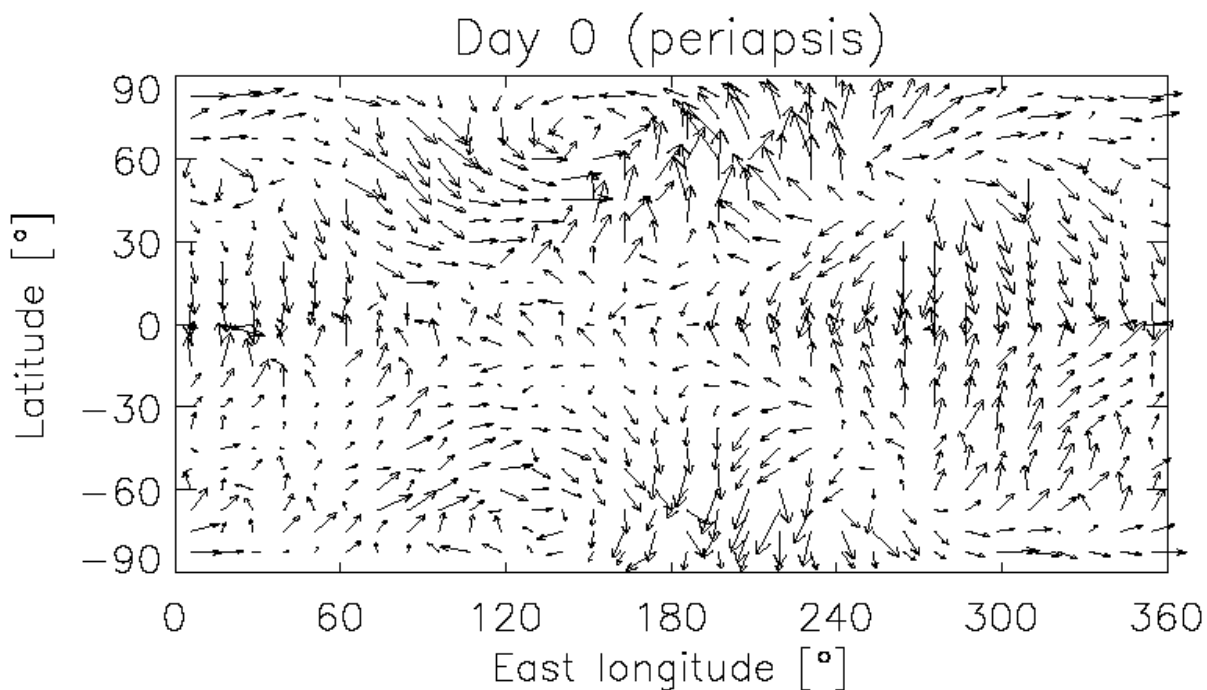


Figure 4-13. TN02 wind field at 300 m (Fig. 5 of TN02).

TN02 only shows simulated global wind fields for altitudes of 300 m and 40 km, hence it is not clear if the wind pattern for altitudes below 40 km will be well described by the approximation used in this study.

4.4. Random Wind Component

A normal random component with a standard deviation $\sigma = 0.5$ m/s is added to the zonal and meridional components of the wind field. Since these two added random numbers are independent, the standard deviation of the global wind field with a random component is $\sigma = 1$ m/s. The value of standard deviation $\sigma = 1$ m/s is consistent with the Huygens probe observations of the Titan winds in the lower atmosphere and with TN02 GCM simulations.

Implementing randomization in a similar fashion as that used in Titan-GRAM 2004⁶ was considered and rejected, because Titan-GRAM generates random winds with magnitudes up to 7-9 m/s in the lower 20 km of the atmosphere. These wind magnitudes are inconsistent with Huygens observations and would be larger than the magnitudes of the background zonal and tidal winds. The resultant global wind field dominated by random winds would produce balloon motions resembling “Brownian motion”.

⁶ C.G. Justus, A. Duvall, D.L. Johnson, “Engineering-level Model Atmospheres for Titan and Neptune”, AIAA 2003-4803, 39th AIAA/ASME/SAE/ASEE Joint Propulsion Conference and Exhibit, 20-23 July 2003, Huntsville, Alabama

4.5. Parametric Models Wind Fields

Figure 4-14 and Figure 4-15 show vector plots of the global wind field in the parametric model with TN05 zonal winds at 8 km and for seasons $L_s=180^\circ$ and $L_s=270^\circ$. These plots illustrate the nature of the global wind field in this parametric model.

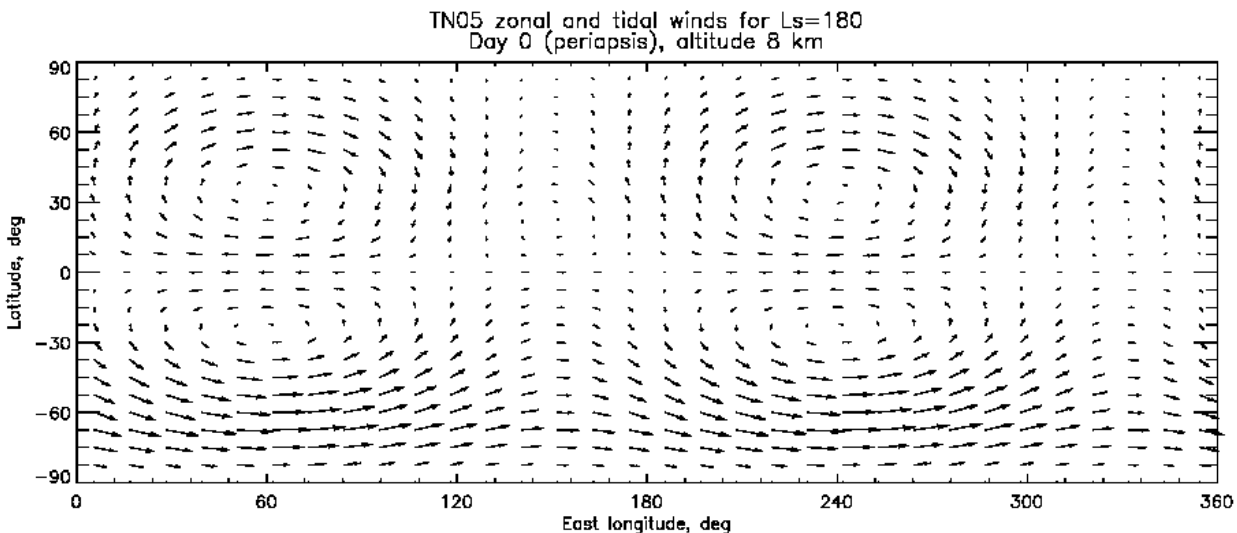


Figure 4-14. Global wind field at 8 km $L_s=180^\circ$ in the parametric model with TN05 zonal winds.

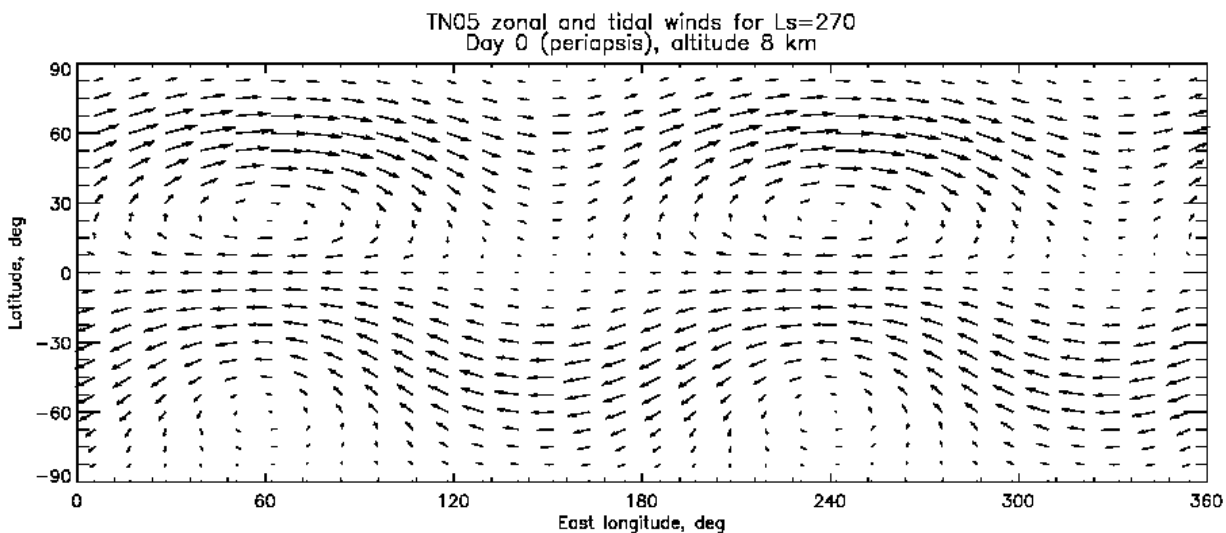


Figure 4-15. Global wind field at 8 km $L_s=270^\circ$ in the parametric model with TN05 zonal winds.

For comparison, Figure 4-16 shows the global wind field in the parametric model with LMD zonal winds at 8 km and for $L_s=270^\circ$. As can be seen, the tidal winds affect the global wind pattern to a much lesser extent in this case, than in the case of the parametric model with TN05 zonal winds.

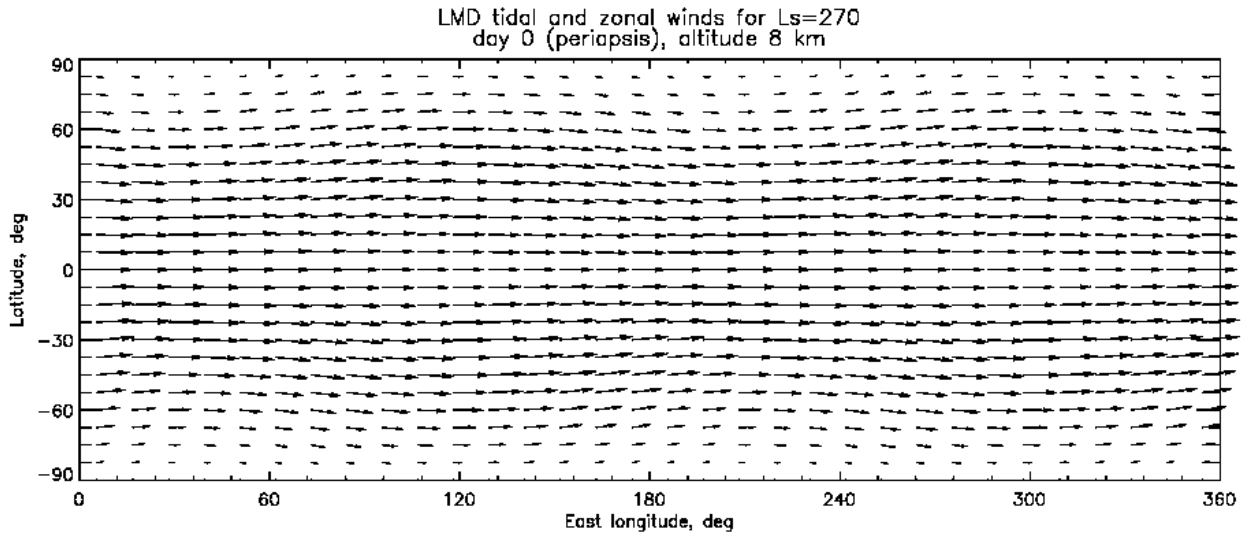


Figure 4-16. Global wind field at 8 km Ls=270° in the parametric model with LMD zonal winds.

5. Trajectory Simulation Results

5.1. Introduction

This section presents the results of the trajectory simulations in the lower atmosphere of Titan and answers the three main questions of the study, namely, to determine 1) whether the trajectories are very similar to each other, 2) whether the trajectories generally cover a wide or narrow range of locations (latitudes), and 3) whether the trajectories appear to be entirely trapped within a narrow region (e.g., near the pole if started at high latitudes). Altogether 9,240 simulated trajectories were generated. The raw data and plots of the simulated trajectories are delivered with this report on a set of 9 CD-ROMs.

5.2. Trajectory Similarity

The simulated trajectories are not similar to each other. The patterns of the simulated trajectories strongly depend on zonal wind model, altitude, starting latitude and season (See Figure 5-1 and Figure 5-2 for example). The variations in the patterns of trajectories are explained by the interplay between the tidal winds and the zonal winds. When the magnitude of the zonal winds is smaller or comparable to the magnitude and direction of the phase velocity of the tidal planetary-scale wave (at a given latitudinal range), the simulated trajectories are strongly affected by the tidal winds. They tend to show loops, zigzags and, in general, cover a wide range of latitudes. Such trajectories are observed primarily among the trajectories simulated with the parametric model with TN05 zonal winds. In the opposite case when the magnitude of the zonal wind is stronger than the magnitude of the phase velocity of the tidal planetary-scale wave, the simulated trajectories are weakly affected by the tidal winds. The simulated balloons tend to pass quickly through the varying field of the tidal winds and the tidal effects are “averaged out” along simulated trajectories. As a result, the simulated trajectories do not show loops and cover a narrow range of latitudes. Such trajectories are observed primarily among the trajectories simulated with the parametric model with LMD zonal winds.

5.3. Range of Locations (Latitudes)

Figure 5-1 shows simulated trajectories for $L_s=270^\circ$ and altitude of 18 km generated with the parametric model with TN05 zonal winds. The figure shows seven color-coded trajectories generated for different starting latitudes (see figure legend). These trajectories represent a subset of 12 random trajectories generated for each starting latitude (-65° , -45° , -25° , 0° , 25° , 45° , 65°). Cross-marks indicate 30-Earth day timestamps. As the zonal winds at this altitude and season (0-2 m/s, see Figure 4-3) are comparable to the phase velocity of the tidal wind planetary-scale wave (0-6 m/s) the trajectories show loops, bends and cover a modest range of latitudes (30° - 50°) depending on initial conditions. In some instances (for example, for starting latitude of -45°) trajectories cover a narrow longitudinal range due to weak zonal winds at this latitude.

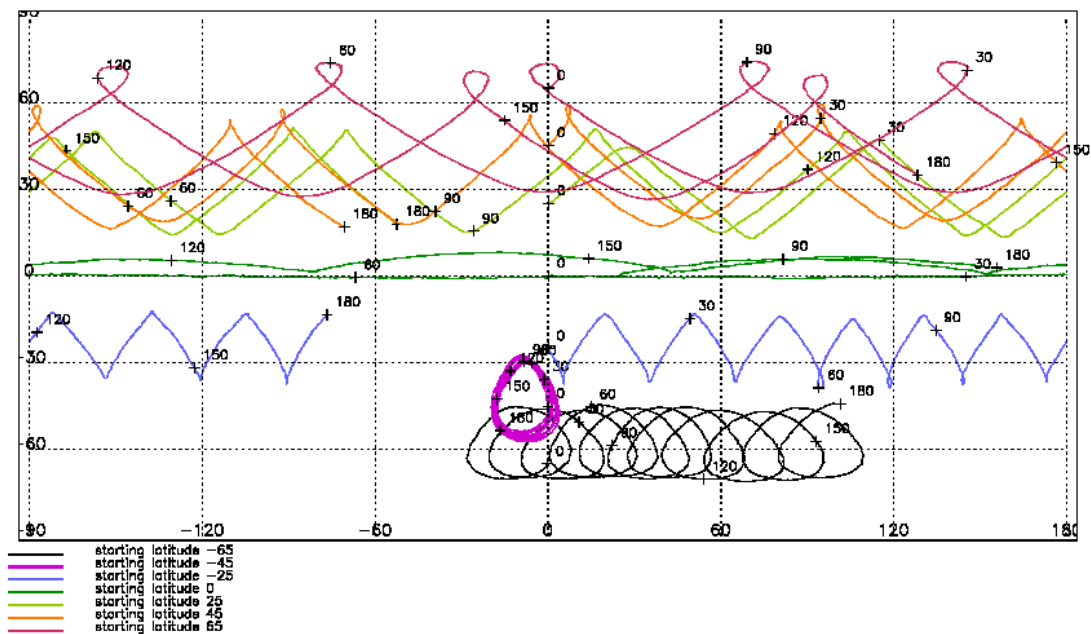


Figure 5-1. Simulated trajectories at 18 km, $L_s=270^\circ$ generated with parametric model with TN05 zonal winds.

Figure 5-2 shows simulated trajectories for $L_s=270^\circ$ and altitude of 18 km generated with the parametric model with LMD zonal winds. Different segments of 180-Earth day trajectories shown in Figure 5-2 completely overlap and cannot be distinguished in the figure. The trajectories are quite different from the trajectories shown in Figure 5-1. They do not show loops or zigzags and cover a narrow range of latitudes (10° - 20°). This is due to LMD zonal winds at this altitude (5-25 m/s) being larger than the phase velocity of the tidal wave (0-6 m/s).

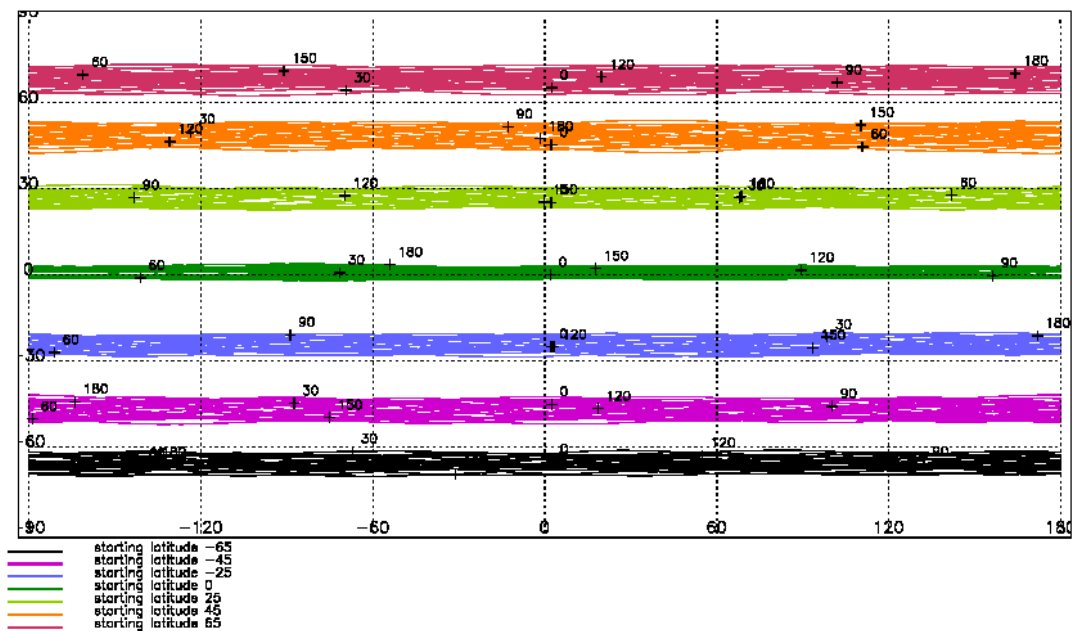


Figure 5-2. Simulated trajectories at 18 km, $L_s=270^\circ$ generated with parametric model with LMD zonal winds.

At low altitudes in the LMD model, where the zonal winds become weaker, we see similar, but different patterns of trajectories as generated with the TN05 model (see Figure 5-3).

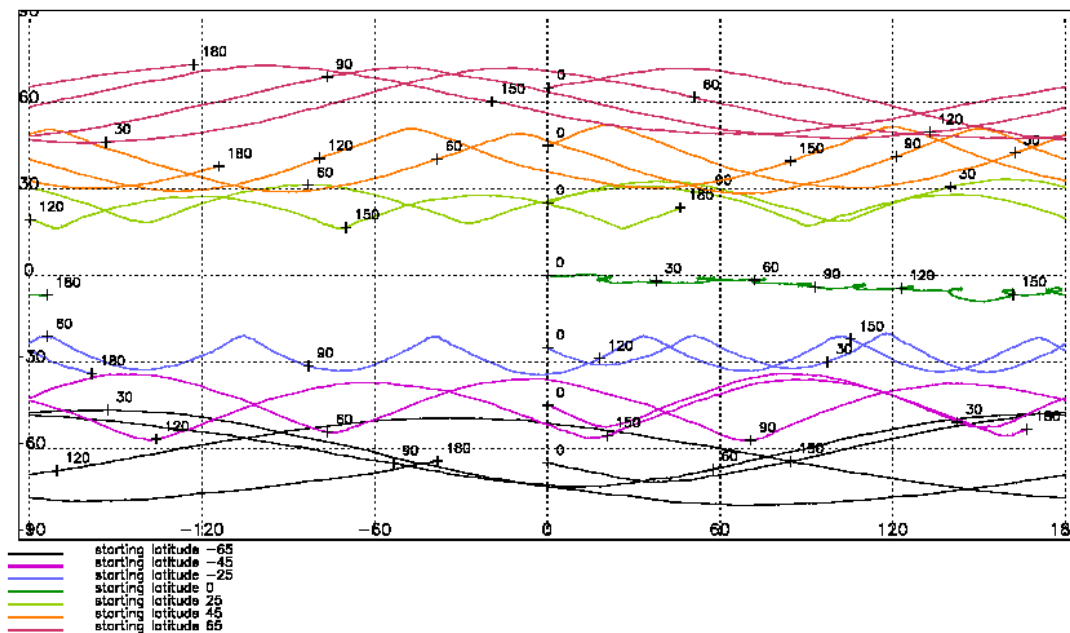


Figure 5-3. Simulated trajectories at 1 km, Ls=270° generated with parametric model with LMD zonal winds.

The evolution of the shape of a simulated trajectory with varying background zonal and tidal winds can be observed in Figure 5-4. The plot shows nine color-coded simulated trajectories at 18 km each 32-Earth days long and each with a starting latitude of -65°. Cross-marks indicate 4-day timestamps.

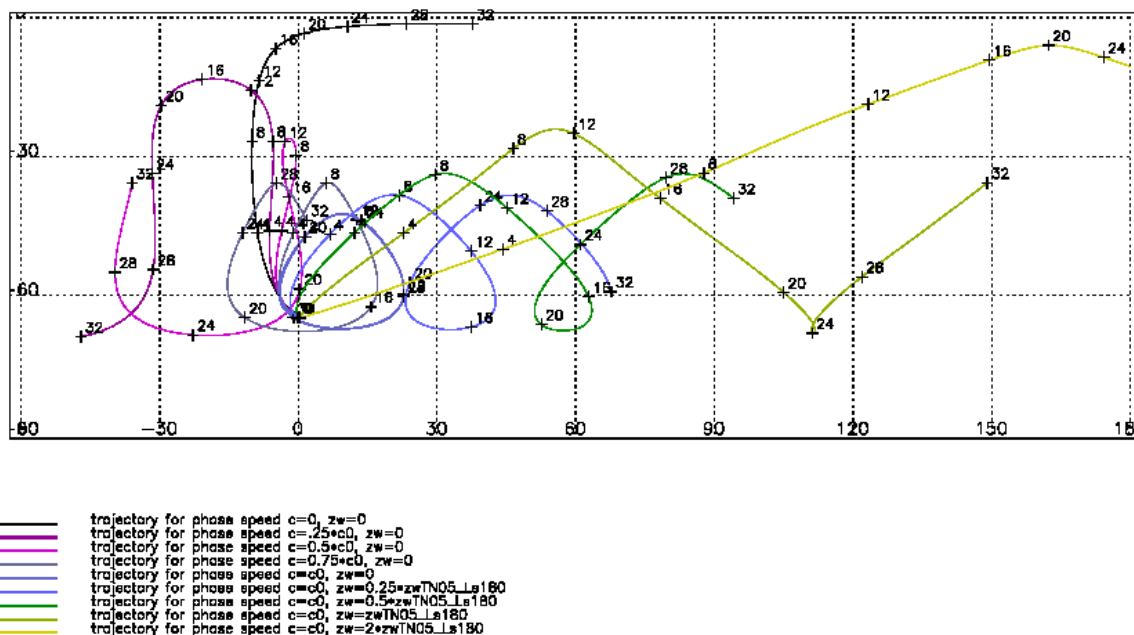


Figure 5-4. Evolution of the shape of a trajectory with varying underlying winds.

Each trajectory is simulated in different background zonal and tidal wind field. The first trajectory (black) is simulated with the phase speed of the tidal wind planetary wave and the background zonal winds set to zero. This trajectory has the maximum meridional extent. The next four trajectories (see figure legend) are simulated with the background zonal winds set to zero and the phase speed of the tidal wind wave increasing gradually to its actual value. As the phase speed is being increased, the meridional extent of the simulated trajectory decreases, as it “sees” both negative and positive tidal meridional winds. The net displacement changes from being westward for small phase speeds, to being eastward for normal phase speed.

The next four trajectories are simulated with the background zonal winds of the TN05 model at 18 km for $L_s=180^\circ$ increasing gradually from a quarter to twice their actual magnitude. The zonal winds at this altitude and latitude for this season are prograde – in the same eastward direction that the tidal wind wave propagates. Hence, if the zonal winds match the magnitude of the phase speed of the tidal wind wave, the balloon is stationary relative to the moving spatial pattern on the tidal winds. Consequently, as the zonal wind speeds are increased, the meridional extent of the trajectory increases.

Trajectories in Figure 5-4 show most of the types of patterns observed in the simulations (except for those in high zonal winds – see Figure 5-2).

Figure 5-5 is a 3-D chart that displays five simulated trajectories generated with the parametric model with TN05 zonal winds for the same starting latitude of 65° , but at different altitudes. The vertical scale is altitude in km. Cross-marks again mark 30-Earth day intervals. This plot demonstrates variability of simulated trajectories with altitudes as the zonal winds vary with altitude (the tidal winds also vary with altitude as amplitudes u_{0t} and v_{0t} vary, but these variations are smaller than the variations in the zonal winds).

TN05 zonal winds, Ls=270
 Starting latitude: 65
 Random component std=1 m/s

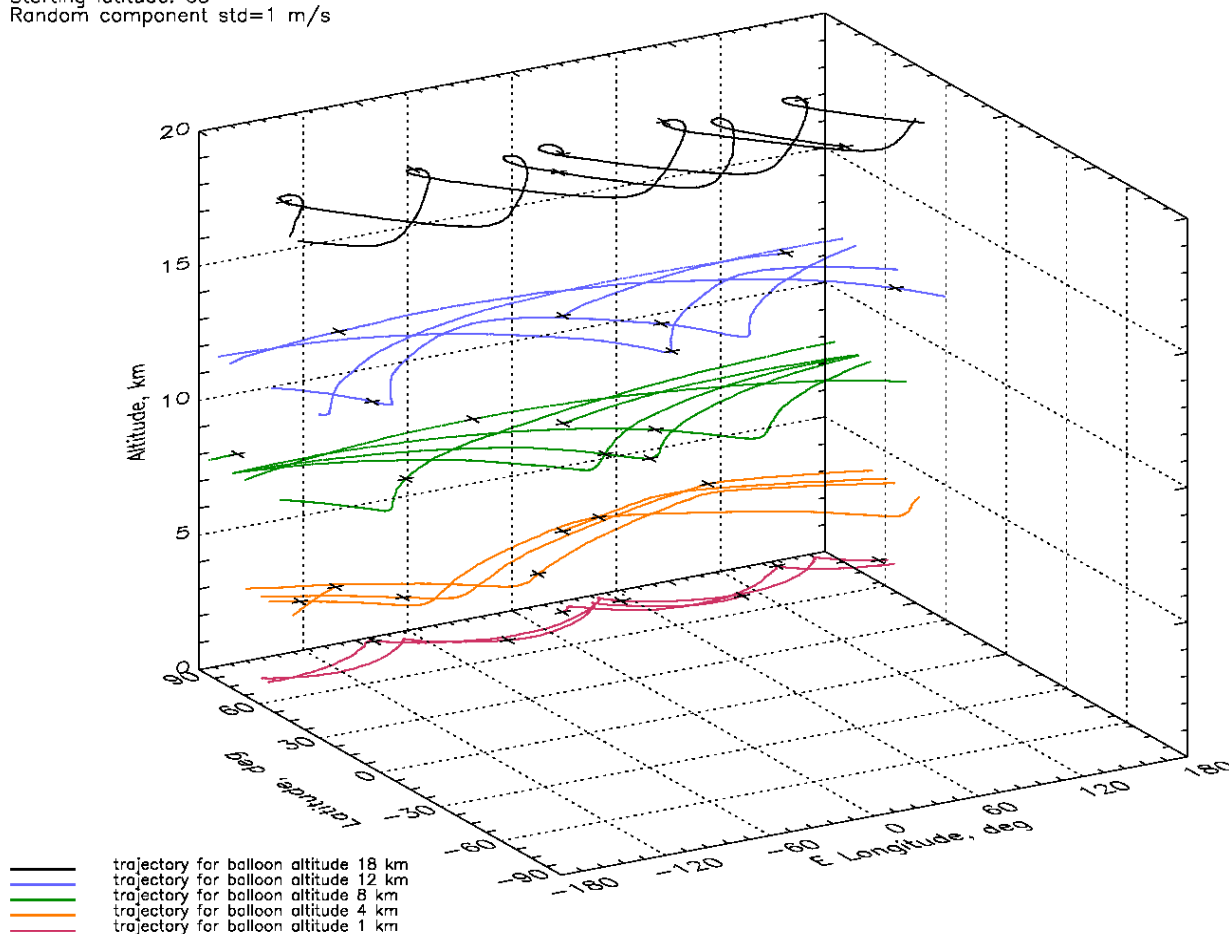


Figure 5-5. Simulated trajectories at altitudes of 1, 4, 8, 12 and 18 km, Ls=270°, starting latitude of 65° generated with parametric model with TN05 zonal winds.

Daily variations in wind field, simulated by generating trajectories at different local hours, seem to produce more variability than random variations of the wind field with $\sigma = 1$ m/s. Compare, for example, Figure 5-6 to the trajectory originating at latitude of -65° in Figure 5-1. Figure 5-6 shows 12 simulated trajectories initiated at different local hours spanning one Titan day, for Ls=270°, altitude of 18 km and parametric model with TN05 zonal winds. While the general appearance of the trajectory does not change significantly, trajectories generated at different local hours do cover different portions of the planet.

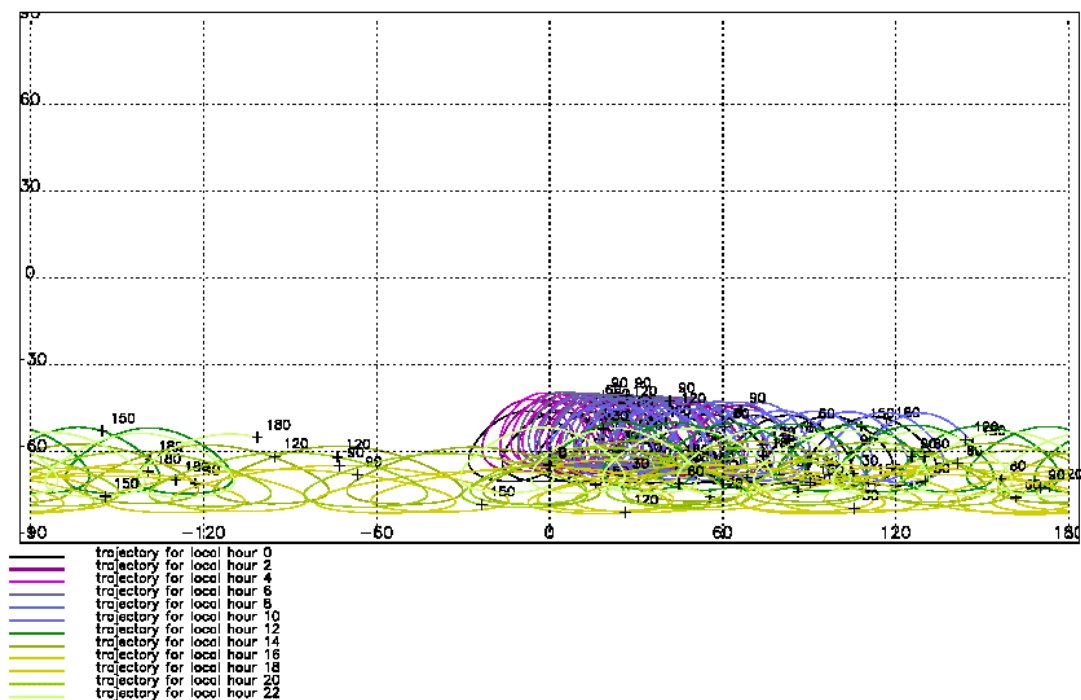


Figure 5-6. 12 trajectories simulated for different starting local time, for $L_s=270^\circ$, 18 km altitude, parametric model with TN05 zonal winds.

Not all of the trajectories circumnavigate the Titan, as can be seen in Figure 5-1. Some of the trajectories cover not just a limited range of latitudes, but also a limited range of longitudes. Figure 5-7 shows longitudinal envelopes of trajectories generated for different initial latitudes and local times at $L_s=180^\circ$, 18 km altitude, parametric model with TN05 zonal winds. The longitudinal envelopes mark the maximum and the minimum latitude observed in the set of 12 trajectories initiated at the same latitude for any given longitude. As can be seen in the figure, simulated trajectories in high latitudes in the Northern hemisphere do not circle Titan over a 180-Earth day time period. The combination of zonal and tidal winds produces global winds that are not strong enough to drive the balloon around Titan in 180 Earth days (~ 11 Titan days). It is also interesting to note that in this particular example simulated trajectories initiated at the latitude of 25° (green) show a lot of variability in latitudinal range depending on longitude. While simulated trajectories cover about 40° of latitudes (from 10° to 50°) for longitudes from 0° to about -150° , for other longitudes the latitudinal coverage is narrow – about 20° (from 10° to 30°). This is apparently due to simulated trajectories passing near the boundary of two dynamically distinct flow regions (zonal winds blowing in different directions) and are being pushed into a separate flow region by random perturbations in the wind field.

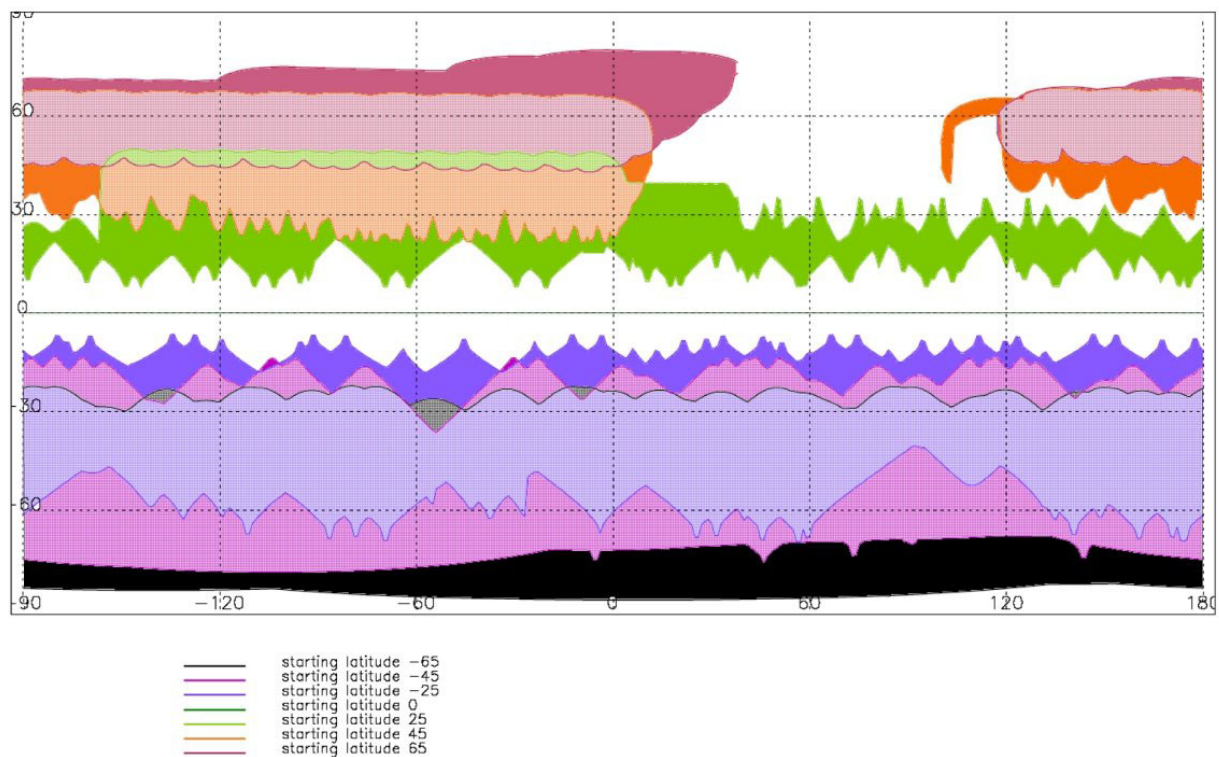


Figure 5-7. Longitudinal envelopes of sets of trajectories initiated at different latitudes and different local times at $L_s=180^\circ$, 18 km altitude, parametric model with TN05 zonal winds.

The ranges of the latitudes covered by simulated 180-Earth days trajectories were analyzed by plotting histograms of latitudes for all altitudes and seasons for both parametric models. Figure 5-8 illustrates this analysis. Figure 5-8 shows 7 histograms of latitudinal coverage for the groups of 12 random trajectories generated for 7 starting latitudes and $L_s=270^\circ$, 18 km altitude with the parametric model with TN05 zonal winds. The latitudinal extent of the coverage ranges from 22° for the trajectories started at 0° latitude, to 53° for the trajectories started at 65° latitude. It is interesting to note that all of the histograms, with the exception of the histogram for trajectories starting at 0° latitude, are clearly bimodal. The picks in the latitudinal histograms correspond to simulated balloons spending more times at some latitudes due to meridional and zonal winds being weaker at these latitudes.

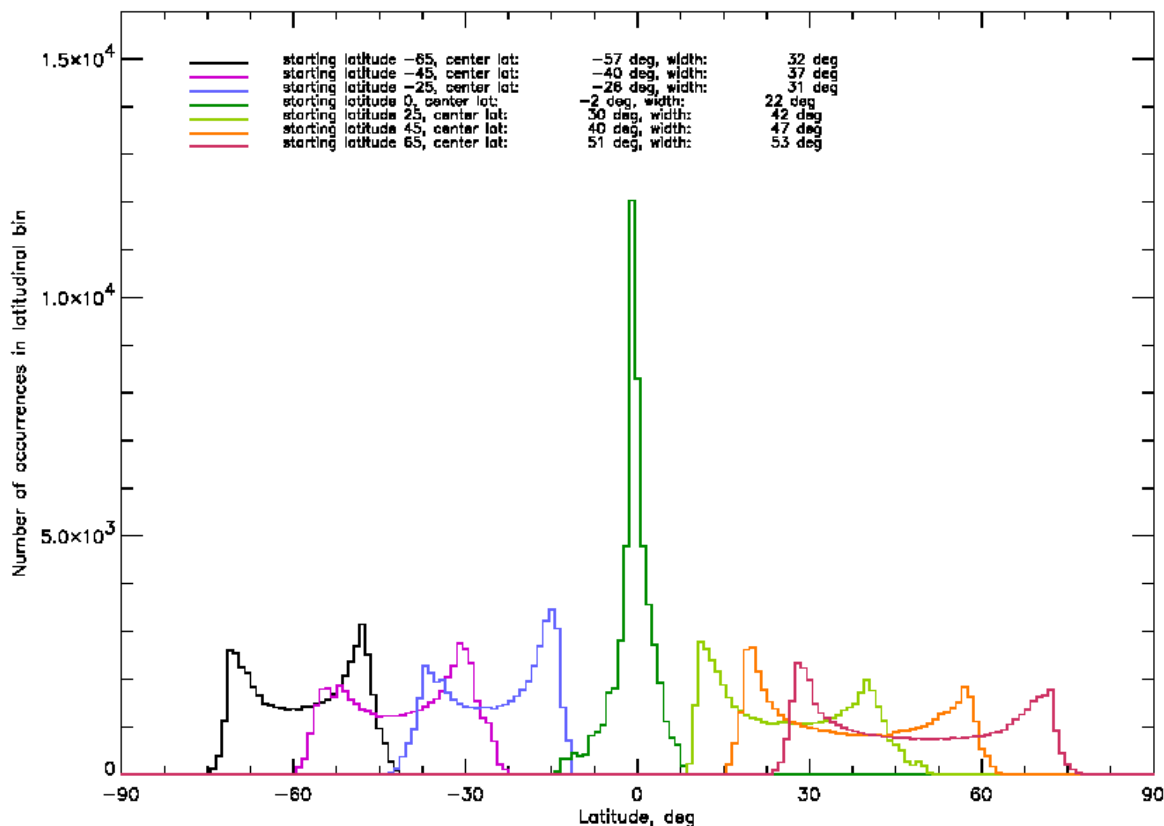


Figure 5-8. Histograms of latitudes covered by simulated trajectories generated with TN05 zonal wind model with random component for $L_s=270^\circ$, 18 km altitude.

Figure 5-9 shows the same histogram analysis, but for 12 trajectories generated at different local times for the same starting latitude. Trajectories initiated at 0° latitude remain at that latitude because the magnitude of the tidal winds is equal to 0 at the equator at all altitudes in the parametric model and there is no random component in simulations that vary the local hour of the simulation start time. Histograms shown in Figure 5-9 do not exhibit bimodality, as the histograms of random trajectories do (Figure 5-8). They also cover wider latitudinal ranges – from 40° to 70° (with the exception of the trajectories starting at 0° latitude).

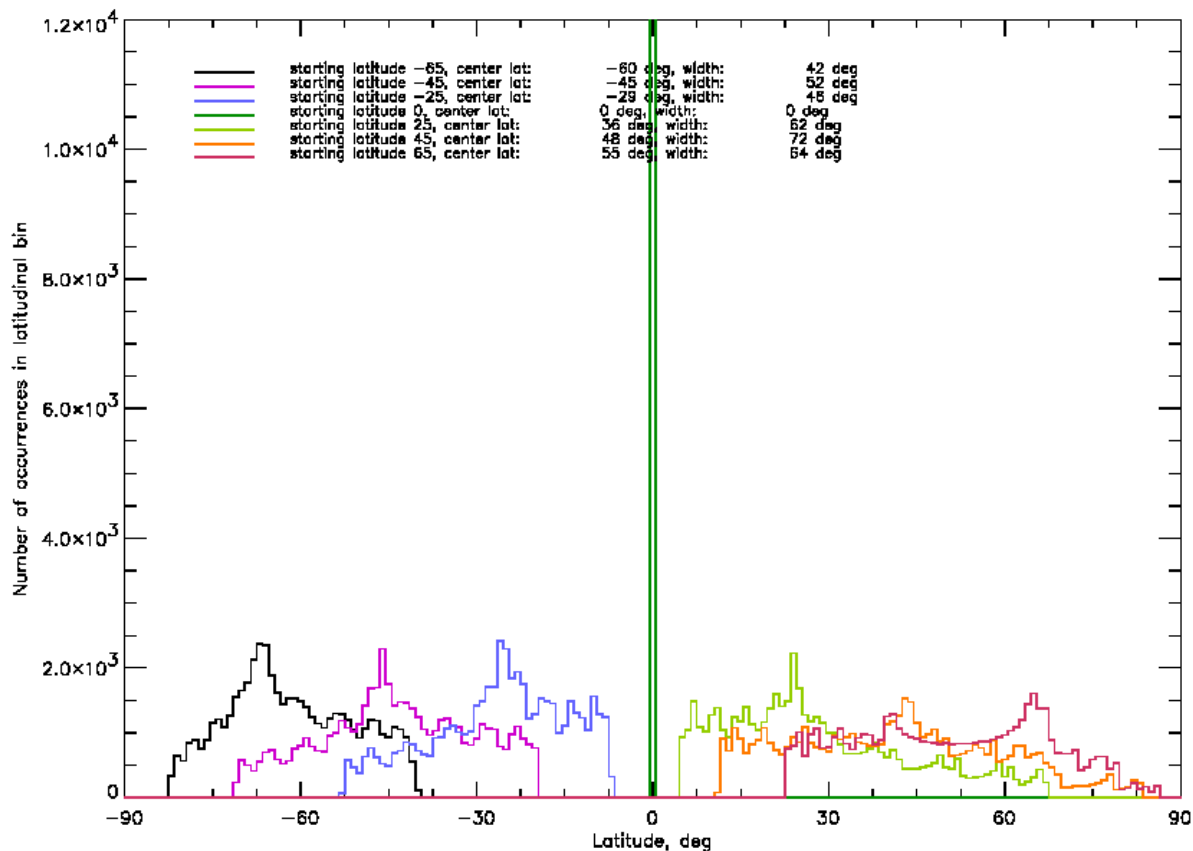


Figure 5-9. Histograms of latitudes covered by simulated trajectories generated for 12 different local hours with TN05 zonal wind model for $L_s=270^\circ$, 18 km altitude

Figure 5-10 shows the histogram plot for the conditions of Figure 5-8, but for parametric wind model with the LMD zonal winds. As was noted before, strong zonal winds in the LMD model minimize the effects of tidal winds and the simulated trajectories cover narrow ranges of latitudes (at altitudes above 4 km). The latitudinal ranges covered by simulated trajectories in Figure 5-10 range from 10° for trajectories started at 0° latitude to 18° for trajectories started at 65° latitude. The histograms are not bimodal, again due to strong zonal winds that minimize any effects of the tidal winds.

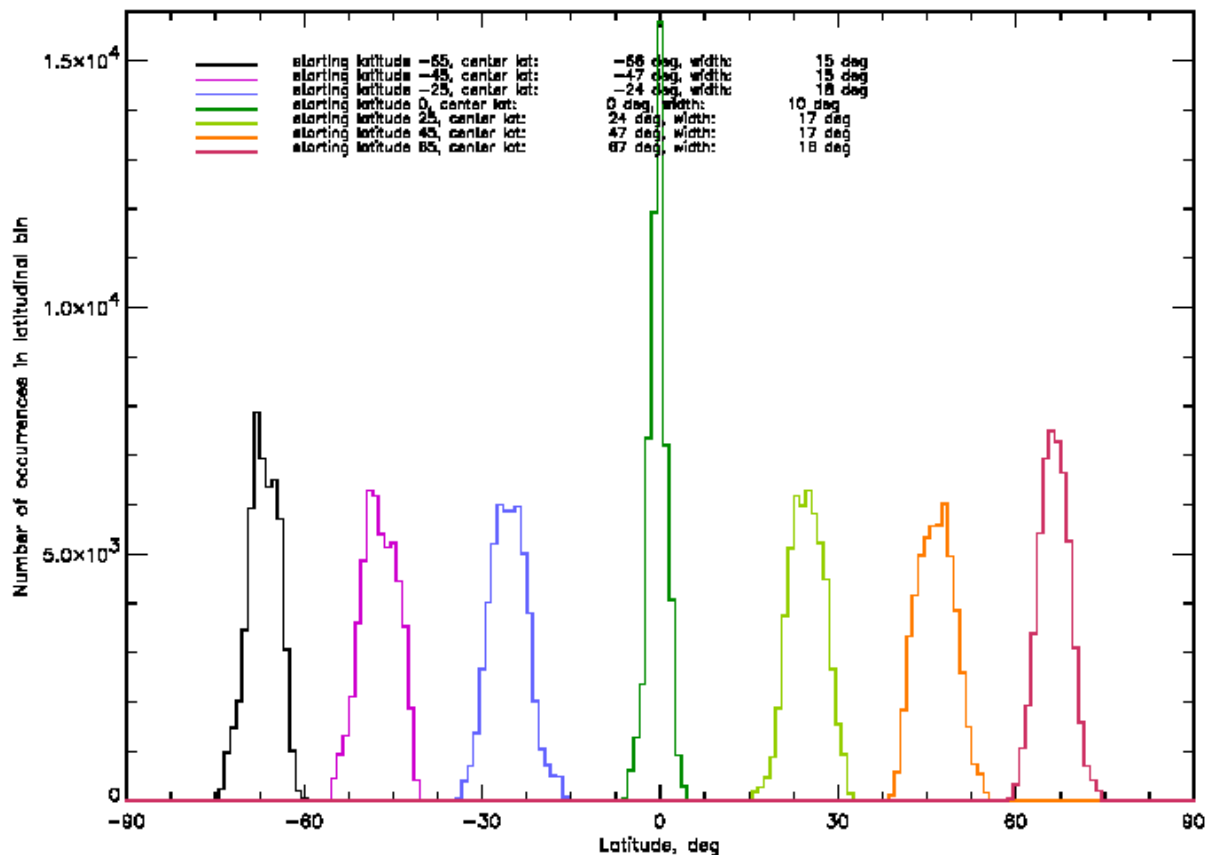


Figure 5-10. Histograms of latitudes covered by simulated trajectories generated with LMD zonal wind model with random component for $L_s=270^\circ$, 18 km altitude.

Figure 5-11 summarizes the histogram analysis for random trajectories for all altitudes for the season of $L_s=270^\circ$ and parametric model with the TN05 zonal winds. The plot displays the latitudinal extent of the histograms for five altitude levels (1, 4, 8, 12 and 18 km). The vertical bars indicating latitudinal extent of the histograms are offset in horizontal direction (altitude axis) so that the symbols for latitude limits do not overlap. Colored squares indicate central latitude of the histogram (color coding corresponds to that on Figure 5-8-Figure 5-10). As can be seen in Figure 5-11, trajectories in high northern latitudes (45° - 65°) have the largest latitudinal extent at all altitudes, except at 1 km. This is due to relatively strong prograde zonal winds centered at about 60° latitude characterizing circulation during this season in TN05 zonal wind model. As was noted before, prograde zonal winds with magnitudes comparable to the magnitude of the phase speed of the tidal wind planetary wave amplify tidal wind effects (meridional excursion in this case).

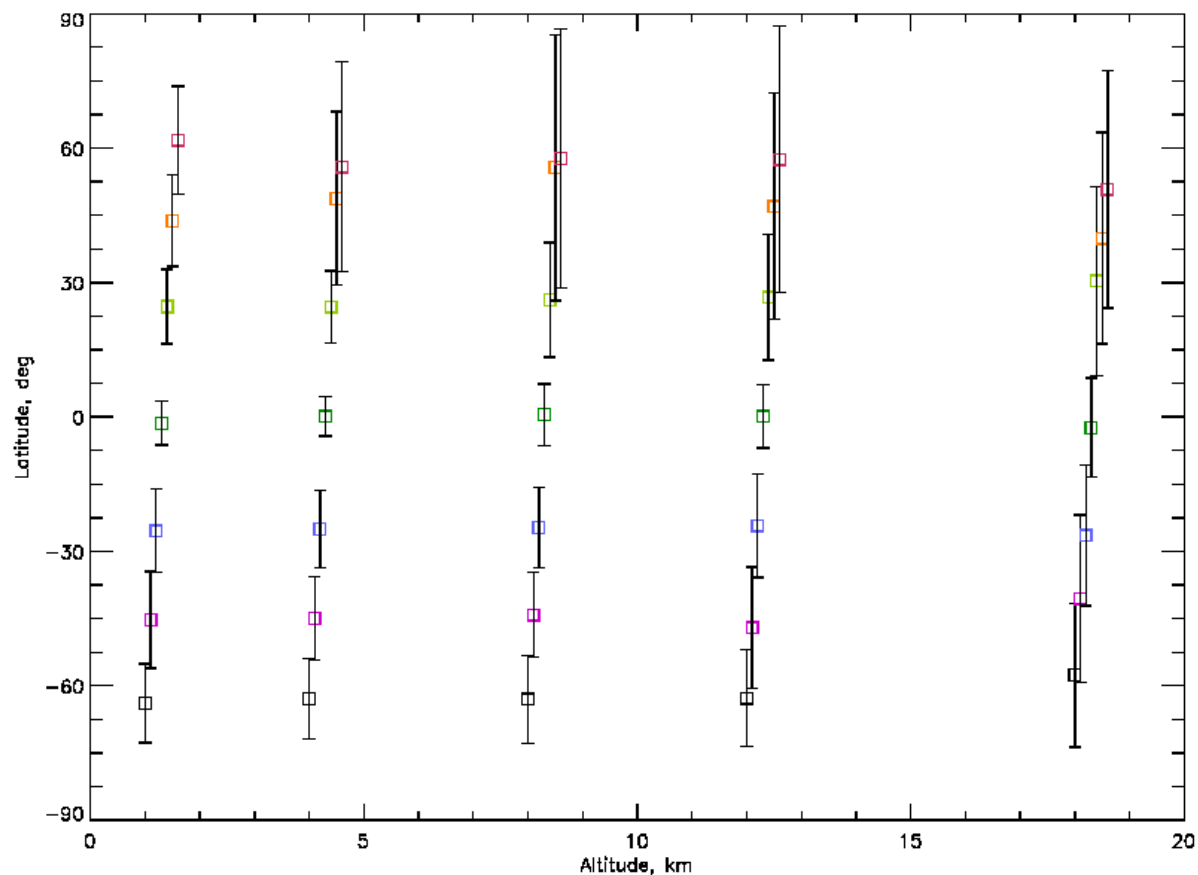


Figure 5-11. Latitudinal ranges at different altitudes covered by simulated trajectories generated with TN05 zonal wind model with random component for $L_s=270^\circ$.

Figure 5-12 shows analysis similar to that in Figure 5-11, but for trajectories simulated at different local hours. The latitudinal ranges covered by trajectories in this case are wider than in Figure 5-11, but show the same tendency to be wide in the Northern hemisphere.

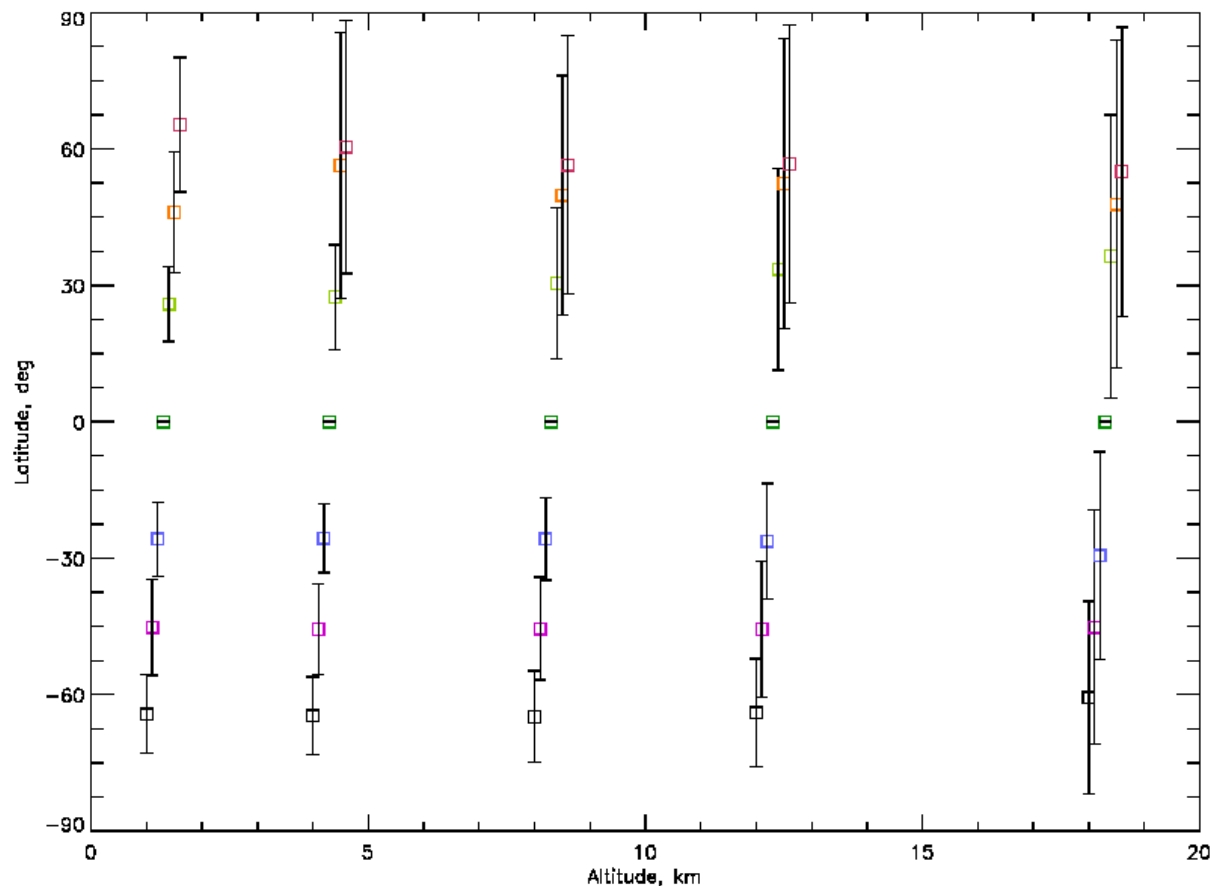


Figure 5-12. Latitudinal ranges at different altitudes covered by simulated trajectories generated for 12 different local hours with TN05 zonal wind model for $L_s=270^\circ$.

Figure 5-13 displays the histograms of latitudinal coverage for all trajectories generated with parametric model with TN05 zonal winds and with the LMD model for seasons corresponding to $L_s=180^\circ$, 270° and 0° (zonal winds do not change significantly in the LMD model, hence the variability in the latitudinal coverage of simulated trajectories is well reproduced with data for this three seasons). The top plot in Figure 5-13 shows the histograms for parametric model with TN05 (solid line) and LMD (dashed line) zonal winds and random trajectories; the plot at the bottom of Figure 5-13 shows histograms for trajectories generated at different local hours. The width of the histograms bins is 4° of latitude (except for the first bin, which is 2° wide). Each data point indicates how many times a given latitudinal range is observed in all the histograms of latitudinal coverage (Figure 5-8 - Figure 5-10). For example, the top plot indicate that latitudinal extent of 14° to 18° (histogram bin 5) is observed 32 times in histograms of latitudinal extent of simulated trajectories generated with parametric model with TN05 zonal winds. These histograms indicate that weak zonal winds (TN05 zonal model) tend to produce trajectories that, in general, cover wider range of latitudes than trajectories simulated with strong zonal winds (LMD).

Interestingly, for both zonal wind models and for both random and local hour varying trajectories the most often occurring range of covered latitudes is about the same: between 10° and 18° (bins 4 and 5 of histograms in Figure 5-13). This means that the most probable latitudinal range of simulated trajectories is 10° and 18° , independent of the wind model.

Maximum latitudinal range observed in this study is 80° for simulations with random trajectories and LMD zonal winds, and 70° for simulations with varying local time and TN05 zonal winds.

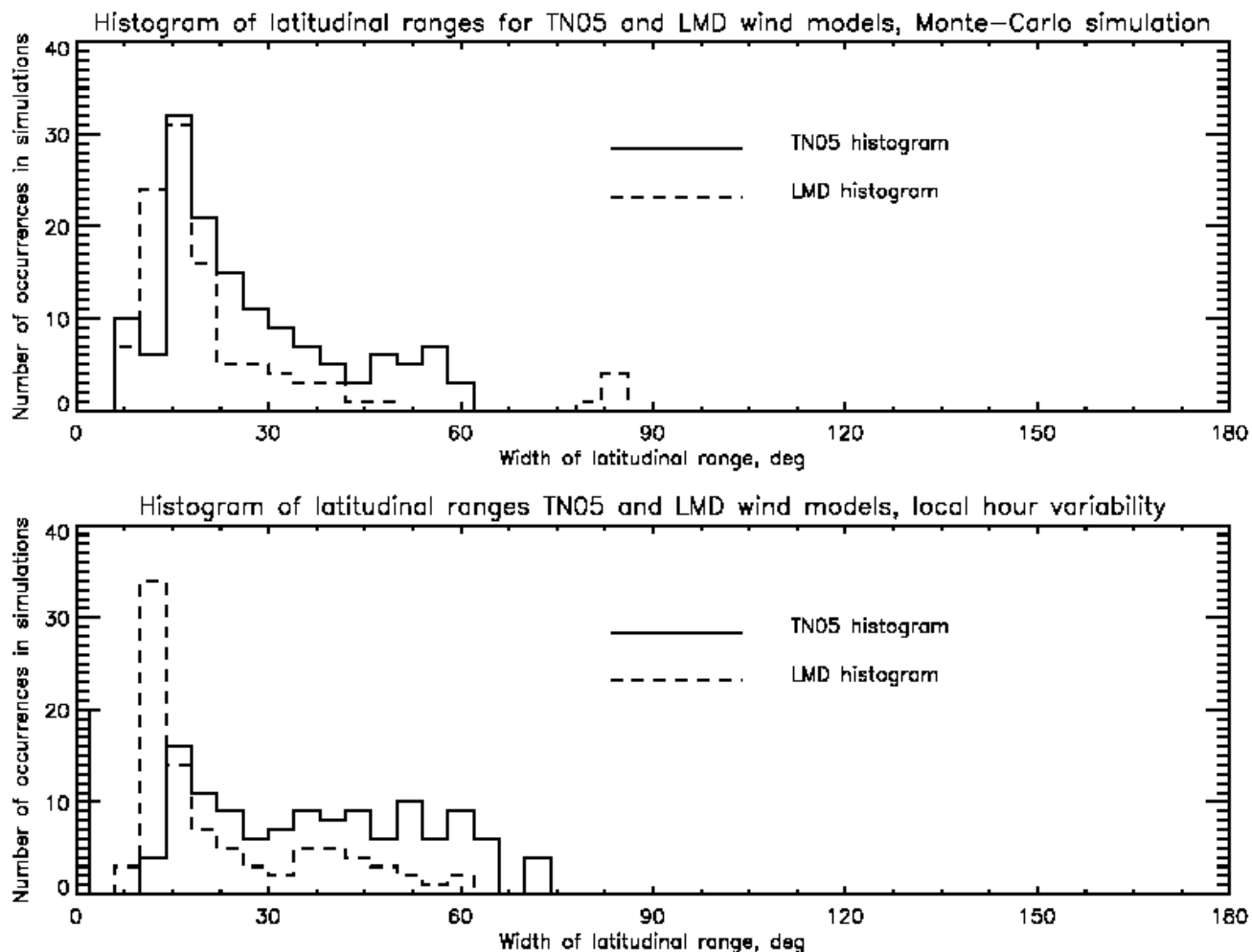


Figure 5-13. Histograms of latitudinal ranges for all altitudes and seasons, for both parametric models (top) for simulations with 12 random trajectories for each starting latitude; (bottom) for simulations with trajectories at 12 different local hours for each starting latitude.

In the parametric wind model with the LMD zonal winds, the widest latitudinal range is observed for simulated trajectories at 4 km altitude and in the equatorial regions (for all seasons and for both random trajectories and for trajectories with varying initial local hour). This is because the zonal winds at 4 km in the equatorial regions in the LMD model have a magnitude that is close to the magnitude of the phase speed of the tidal planetary wave. This point is illustrated in Figure 5-14. Figure 5-14 displays the magnitude of the tidal wave phase speed as a function of the latitude, and magnitudes of the zonal winds in the LMD model for $L_s=270^\circ$ at different altitudes. The magnitude of the tidal-wind, planetary-wave phase speed is the closest to the magnitude of the zonal winds in the equatorial regions at 4 km altitude, and this is the altitude and the latitudes where we see the maximum latitudinal range by the simulated trajectories. Zonal winds at the higher altitudinal level used for simulation in this study (8 km) are stronger than the phase speed at all latitudes, and zonal winds at lower altitudinal level (1 km) are weaker than the phase speed

(except near the poles), - the latitudinal extent of the simulated trajectories at these altitudes is smaller.

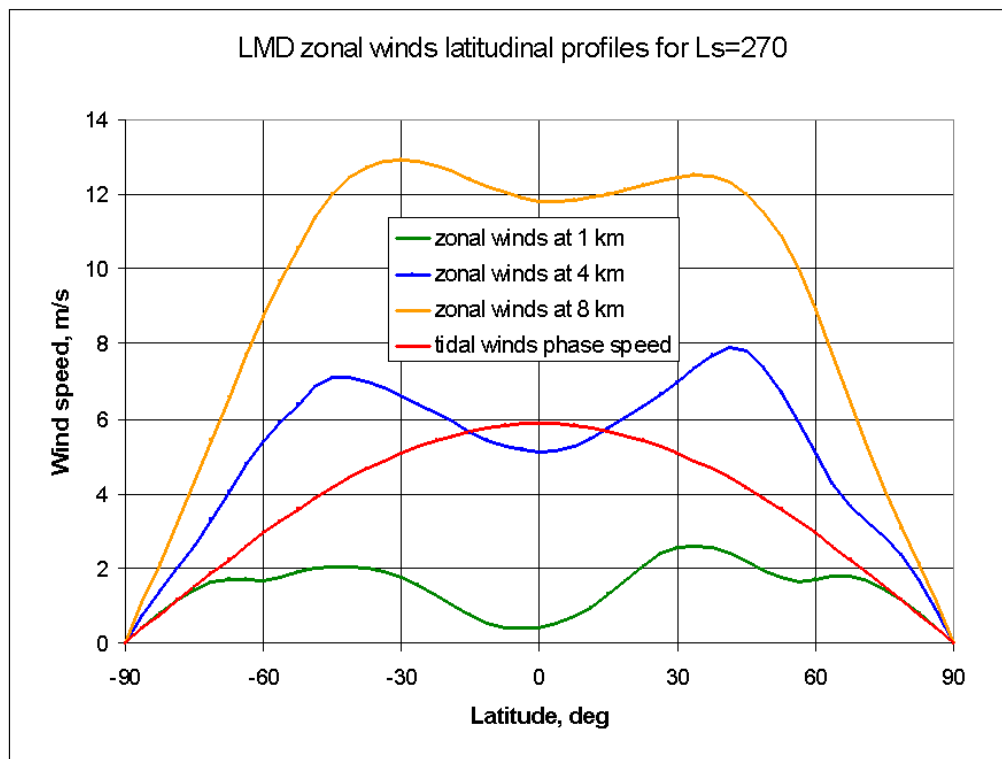


Figure 5-14. Comparison of zonal wind magnitudes in the LMD model for $L_s=270^\circ$ and phase speed magnitude of the tidal wind planetary wave.

For comparison with Figure 5-14, Figure 5-15 shows the comparison of zonal wind and tidal wind planetary wave magnitudes for the same season for the TN05 zonal wind model. As can be seen from the figure, the magnitudes of the zonal winds and of the tidal wind planetary wave phase speed are the closest in high latitudes of the Northern hemisphere almost at all altitudes. Consequently, we see the largest latitudinal coverage by simulated trajectories at these latitudes in TN05 model for $L_s=270^\circ$ (see Figure 5-11 and Figure 5-12). As the zonal circulation changes more significantly with season in TN05 model than in LMD model, the altitudes and latitudes where simulated trajectories show maximum latitudinal coverage change with the season for TN05 model.

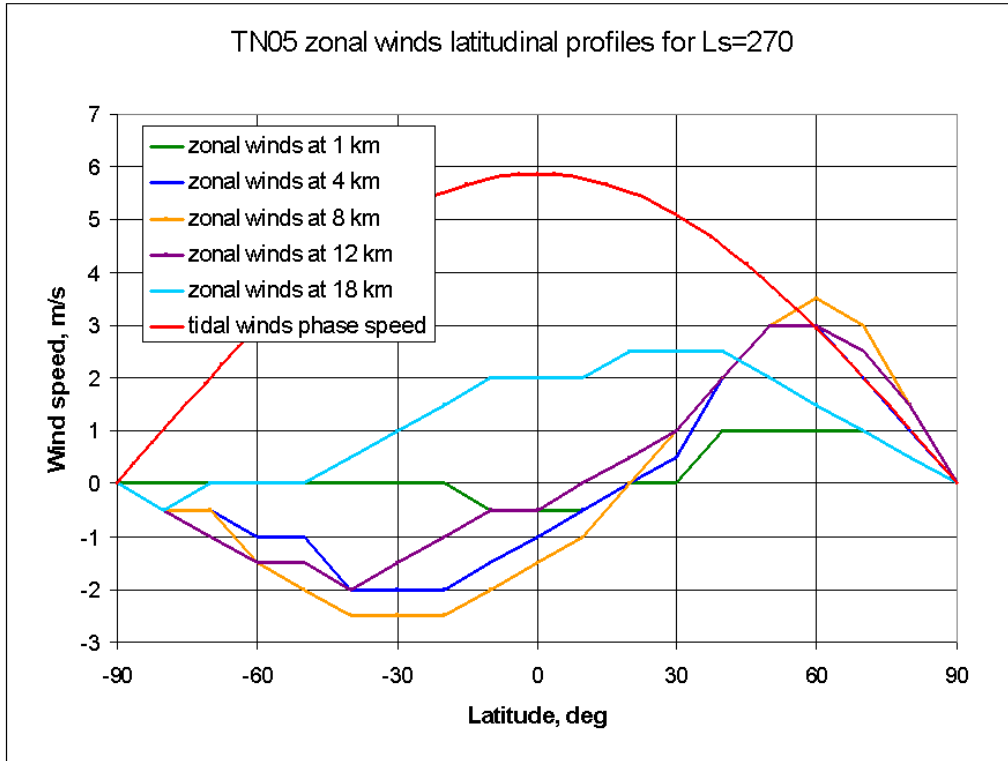


Figure 5-15. Comparison of zonal wind magnitudes in the TN05 model for Ls=270° and phase speed magnitude of the tidal wind planetary wave.

6. Summary

Balloon trajectories in the lower atmosphere of Titan (1-18 km) were simulated with two different models of background winds that included parameterized tidal effects. Relative to the question of whether the trajectories are very similar to each other, we have found out that trajectories differ in their shape depending on the strength of the zonal winds in the model, covering wider latitudinal range and exhibiting loops and zigzags in the model with weak (0-4 m/s) zonal winds and covering narrow latitudinal range in the model with strong zonal winds (~10 m/s). Relative to the question of whether the trajectories generally cover a wide or narrow range of locations (latitudes), we have found that latitudinal coverage of the simulated trajectories ranges from 10° to 80° of latitude, depending on model, season, altitude and starting latitude, with the average value for the latitudinal coverage at about 30°. Relative to the question of whether the trajectories appear to be entirely trapped within a narrow region, (e.g., near the pole if started at high latitudes), we have found out that most of the simulated trajectories are confined to a latitudinal corridor centered near their starting latitude.

Appendix A: Earth Dates of Titan Seasons

Titan seasons correspond to the following Earth dates:

Ls=180°	4/23/2025
Ls=210°	9/22/2027
Ls=240°	1/9/2030
Ls=270°	3/31/2032
Ls=300°	6/11/2034
Ls=330°	9/5/2036
Ls=360°	1/9/2039
Ls=90°	10/13/2046